Gross primary production responses to warming, elevated CO_2, and irrigation: quantifying the drivers of ecosystem physiology in a semiarid grassland

Edmund M. Ryan[1]*, Kiona Ogle[2,3], Drew Peltier[3], Anthony P. Walker[4], Martin G. De Kauwe[5], Belinda E. Medlyn[6], David G Williams[7], William Parton[8], Shinichi Asao[8], Bertrand Guenet[9], Anna Harper[10], Xingjie Lu[11], Kristina A. Luus[12,13], Sönke Zaehle[12], Shijie Shu[14], Christian Werner[15], Jianyang Xia[16,17], Elise Pendall[6,7]

[1]Lancaster Environment Centre, Lancaster, UK.

[2]School of Informatics, Computing, and Cyber Systems, Northern Arizona University, Flagstaff, Arizona, USA

[3]Department of Biological Sciences, Northern Arizona University, Flagstaff, Arizona, USA

[4]Environmental Sciences Division and Climate Change Science Institute, Oak Ridge National Laboratory, Oak Ridge, Tennessee, USA.

[5]Macquarie University, Department of Biological Sciences, New South Wales 2109, Australia

[6]Hawkesbury Institute for the Environment, Western Sydney University, Penrith, NSW, Australia.

[7]University of Wyoming, Department of Botany, Laramie, WY, USA

[8]Natural Resource Ecology Laboratory, Colorado State University, Fort Collins, CO 80523-1499 USA.

[9]Laboratoire des Sciences du Climat et de l'Environnement, LSCE/IPSL, CEA-CNRS-UVSQ, Université Paris-Saclay, F-91191 Gif-sur-Yvette, France.

[10]College of Engineering, Mathematics, and Physical Sciences, University of Exeter, Exeter, UK

[11]CSIRO Ocean and Atmosphere, PBM #1, Aspendale, Victoria 3195, Australia.

[12]Biogeochemical Integration Department, Max Planck Institute for Biogeochemistry, Hans-Knöll-Str. 10, 07745 Jena, Germany.

[13]Now at: Dublin Institute of Technology, Dublin, Ireland.

[14]Department of Atmospheric Sciences, University of Illinois, 105 South Gregory Street, Urbana, Illinois 61801-3070, USA.

[15]Senckenberg Biodiversity and Climate Research Centre (BiK-F), Senckenberganlage 25, 60325 Frankfurt, Germany.

[16]Department of Microbiology & Plant Biology, University of Oklahoma, Norman, OK 73019 USA

[17]Research Center for Global Change and Ecological Forecasting, East China Normal University, Shanghai 200062, China.

*Corresponding author:

Lancaster Environment Centre,

Bailrigg, Lancaster.

LA1 4YW

UK

Tel: 00 44 (0) 1524 594009

Email: edmund.ryan@lancaster.ac.uk

Keywords: gross primary production, elevated CO_2, warming, multi-factor global change experiment, Bayesian modelling, carbon cycle, grasslands

For submission to: *Global Change Biology*

Abstract

Determining whether the terrestrial biosphere will be a source or sink of carbon (C) under a future climate of elevated CO_2 (eCO_2) and warming requires accurate quantification of gross primary production (GPP), the largest flux of C in the global C cycle. We evaluated six years (2007-2012) of flux-derived GPP data from the Prairie Heating and CO_2 Enrichment (PHACE) experiment, situated in a grassland in Wyoming, USA. The GPP data were used to calibrate a light response model whose basic formulation has been successfully used in a variety of ecosystems. The model was extended by modeling maximum photosynthetic rate (A_{max}) and light-use efficiency (Q) as functions of soil water, air temperature, vapor pressure deficit, vegetation greenness and nitrogen at current and antecedent (past) time scales. The model fit the observed GPP well ($R^2 = 0.79$), which was confirmed by other model performance checks that compared different variants of the model (e.g., with and without antecedent effects). Stimulation of cumulative six-year GPP by warming (29%, P=0.02) and eCO_2 (26%, P=0.07) was primarily driven by enhanced C uptake during spring (129%, P=0.001) and fall (124%, P=0.001), respectively, which was consistent across years. Antecedent air temperature ($Tair_{ant}$) and vapor pressure deficit (VPD_{ant}) effects on A_{max} (over the past 3-4 days and 1-3 days, respectively) were the most significant predictors of temporal variability in GPP among most treatments. The importance of VPD_{ant} suggests that atmospheric drought is important for predicting GPP under current and future climate; we highlight the need for experimental studies to identify the mechanisms underlying such antecedent effects. Finally, posterior estimates of cumulative GPP under control and eCO_2 treatments were tested as a benchmark against 12 terrestrial biosphere models (TBMs). The narrow uncertainties of these data-driven GPP estimates suggest that they could be useful semi-independent data streams for validating TBMs.

Introduction

Gross primary production (GPP) is the largest flux in the global carbon (C) cycle, representing the gross amount of C removed from the atmosphere by plants via photosynthesis at the ecosystem scale (Chapin III et al., 2006). GPP represents the input of C into the terrestrial biosphere, which plays an important role in determining the magnitudes of the flows and stores of C within plants and soil (Beer et al., 2010, Williams et al., 2005). Despite its importance, there remains large uncertainty in global model projections of future GPP – both globally and regionally – under anticipated future levels of CO_2 and warming (Richardson et al., 2013, Arora et al., 2013), and there is an urgent need to determine the causes of these uncertainties (Friedlingstein et al., 2014). Improved accuracy of these model predictions is critical in determining whether the terrestrial biosphere is likely to be a future sink or source of C.

While the responses of net primary production (NPP) to elevated CO_2 (eCO_2) are well-studied, less work has directly evaluated GPP, partly because it is not directly measurable. The few studies that exist on the singular effect of eCO_2 on GPP report a positive effect. For example, Wittig *et al.* (2005) found a ~80% stimulation of GPP for *Populus* trees growing under eCO_2 over a three year period. Likewise, using three years of leaf-level photosynthesis data, Luo et al. (2001) found a ~40% increase in modelled GPP under eCO_2. A stimulation of NPP under eCO_2 suggests a stimulation of GPP if it is assumed that NPP is proportional to GPP (Williams et al., 2005, Waring et al., 1998). A ~20% increase in NPP under eCO_2 is expected in mid-latitudes (Luo et al., 2006), and this should translate into increased GPP. However, semi-arid grasslands exhibit large variation in NPP responses to eCO_2 (0-100%), which is primarily driven by spatial and temporal precipitation variability (Polley et al., 2013). The stimulation of NPP by eCO_2 has been shown to be suppressed if the ecosystem is nitrogen limited (Norby and Zak, 2011). GPP should also be affected by responses of leaf-level photosynthesis at light saturation (A_{sat}), which increases with eCO_2 in trees (~45%), grasses (~35%), shrubs (~20%) and crops (~35%) (Ainsworth and Long, 2005), but scaling from leaf-level A_{sat} to ecosystem-level GPP is fraught with uncertainties (Arp, 1991, McLeod and Long, 1999, Morgan et al., 2001).

Warming affects GPP directly through the effect of temperature on leaf photosynthesis, and indirectly via alterations in nitrogen mineralization and water availability (Ciais et al., 2014, Cox et al., 2000). As with eCO_2, a stimulation of NPP under warming suggests a stimulation of GPP if it is assumed that NPP is proportional to GPP (Williams et al., 2005, Waring et al., 1998). Terrestrial biosphere models (TBMs) predict a reduction in NPP with long-term warming; if warming reaches 3-5 °C by 2100 under a high CO_2 emissions scenario (Collins et al., 2013), global terrestrial NPP may decrease by 15-100% (10–60 PgC/year) (Sitch et al., 2008, Friedlingstein et al., 2006, Roy et al., 2001). Retrospective analyses also show a negative effect of warming on NPP, such as a ~9% decrease in global NPP between 1980 and 2002, which offset the CO_2 fertilization effect (Magnani et al., 2007). However, the magnitude of the GPP and NPP responses to warming varies among biomes, with northern latitudes expected to exhibit the largest increases (Piao et al., 2008, Rustad, 2008, Landsberg and Waring, 1997). At the site level, a meta-analysis of 32 separate warming experiments found a positive effect of warming on NPP for tundra sites, but no effect for temperate forest and grassland sites (Rustad et al., 2001). At the regional level, a surface temperature increase of 2 ^{o}C between 1988 and 2008 in northern latitudes stimulated GPP during the spring and fall (Piao et al., 2008, Rustad, 2008, Landsberg and Waring, 1997).

TBMs assume that the interactive effect of eCO_2 and warming is positive (Luo et al., 2008, Norby and Luo, 2004). Field data from climate change experiments support this for certain years (Dukes et al., 2005), but over multiple years there is growing evidence that the positive interactive response does not exist or is not as strong as models suggest (Dieleman et al., 2012, Shaw et al., 2002). The effects of eCO_2 and warming – whether singular or combined – may be dependent upon precipitation inputs in water-limited ecosystems (Fay et al., 2003, Huxman et al., 2004, Knapp and Smith, 2001, Schwinning et al., 2004). For example, an experiment in a mixed C3/C4 semi-arid grassland found that aboveground NPP was increased by ~80% when annual precipitation was delivered in a few, large rain events compared to more frequent, smaller events (Heisler-White et al., 2008). Recent work has generalized this by considering the effect of past or antecedent conditions on primary production. For example, Ogle et al. (2015) found that event size and antecedent precipitation explained 75% of the variation in aboveground NPP (ANPP) in the same semi-arid grassland. Likewise, antecedent soil water content was a significant predictor of ANPP in a tall grass prairie (Sherry et al., 2008).

We identified three major knowledge gaps with regard to the response of GPP to climate change. First, few climate change experiments have investigated the combined effects of eCO_2 and warming on primary production (Luo et al., 2008). Second, most of the literature on the ecosystem responses of primary productivity to eCO_2 and warming are based on measurements of NPP (as highlighted above); very few evaluate GPP, yet this is critical for constraining predictions of C cycle responses to climate change (Norby and Luo, 2004). Third, while analyses of climate change experiments often report that treatment effects are contingent upon background climate conditions (e.g., Morgan et al. 2011), the effects of antecedent climate conditions are often not evaluated.

To address these knowledge gaps, we measured and analyzed GPP for six years as part of the Prairie Heating and CO_2 Enrichment Experiment (PHACE). The experiment consisted of six treatments, four of which were applied in a full factorial design with CO_2 (ambient vs. elevated) and temperature (ambient vs. warming), and two others involved deep and shallow irrigation applied under ambient CO_2 and temperature. We drew upon this six-year dataset to address three questions: (1) How does GPP respond to the main and interactive effects of eCO_2 and warming in the context of variable precipitation? (2) What environmental and meteorological factors (e.g., soil water content, antecedent conditions) govern potential responses of GPP to climate change? Finally, we illustrate how our modeling approach can be applied to generate more realistic data products for informing TBMs, and we ask: (3) How does the inclusion of antecedent conditions affect the magnitude and uncertainty in such GPP data products? Accurate estimation of uncertainty is essential in model evaluation exercises, and we provide a full accounting of uncertainty in our analyses.

Materials and methods

Site description

The PHACE site is situated near Cheyenne, Wyoming at an elevation of 1930 m, with a semi-arid, temperate climate. Thirty-year mean annual temperature is 8.3°C and precipitation is 378 mm, with ~75% falling during the growing season (Zelikova et al., 2015). The vegetation is a mixed grass prairie, dominated by two C3 grasses, western wheatgrass (*Pascopyrum smithii* (*Rydb.*) *A. Löve*) and needle-and-thread grass (*Hesperostipa comata Trin and Rupr*), and the C_4 perennial grass blue grama (*Bouteloua gracilis* (*H.B.K.*) *Lag*). Live plant cover ranges up to 70% of ground area (Zelikova et al., 2015), and roots extend to 40 cm with 75% of root biomass occurring above 15-cm depth (Carrillo et al., 2014). The soil is a fine-loamy, mixed, mesic Aridic Argiustoll, and biological crusts are not present (Bachman et al., 2010).

Experimental design

The PHACE experiment was set up as an incomplete factorial design consisting of six treatments and five replicate plots (3.4 m in diameter) per treatments (Morgan et al., 2011). Four of the six treatments – abbreviated as ct, cT, Ct, CT – are a full factorial design of atmospheric CO_2 (ambient at 380-400 ppm [abbreviated as 'c'] versus elevated at 600 ppm ['C']) and warming (no warming ['t'] versus heated by 1.5 ^oC in the daytime and 3.0 ^oC in the nighttime ['T']). The increase in atmospheric CO_2 (600 ppm) for the elevated CO_2 plots (Ct and CT) was achieved using Free Air CO_2 Enrichment (FACE) technology (Miglietta et al., 2001). Warming was simulated (cT and CT) by applying a ceramic heater system using a proportional-integral derivative (PID) feed-back loop (Kimball, 2005).

The final two treatments (cts and ctd) involve irrigation applied to ambient CO_2 and no warming plots (shallow ['s'] or deep ['d'] irrigation). In the context of the PHACE study, the main aim of the irrigation treatments was to test the hypothesis that responses to eCO_2 are indirectly due to increases in soil water. As such, water was applied to the cts and ctd plots in an effort to increase their soil water contents to match that of the Ct treatment. In the cts treatment, irrigation was applied when soil moisture fell below 85% of Ct at the 5-25 cm depth: in 2007, five, 18-mm precipitation events were applied (totaling 90 mm); during 2008-2011, three 21-mm events per year (totaling 63 mm each year), and 2012, four 65-mm events (totaling 260 mm) were applied. The total amount of water applied to the ctd plots was the same as the cts plots, but water was only added twice per year (spring and fall), in approximately equal amounts.

Data description

All data were measured in the field from 2007-2012, and consisted of GPP (μmol C m^{-2} s^{-1}), associated air temperature (Tair; ^oC), volumetric soil water content (SWC; m^2/m^2), ecosystem phenology ("greenness"; %), photosynthetically active radiation (PAR; µmol quanta m^{-2} s^{-1}), aboveground plant nitrogen content (N; g m^{-2}), and relative humidity (RH; %); vapor pressure deficit (VPD; kPa) was computed from Tair and RH. GPP data were obtained indirectly as the difference between measurements of net ecosystem exchange (NEE; µmol C m^{-2} s^{-1}) and ecosystem respiration (R_{eco}; µmol C m^{-2} s^{-1}) that were made within two minutes of each other. NEE was measured using a 0.1 m^3 canopy gas exchange chamber by measuring the rate of change of CO_2 concentration for 1 minute (Bachman et al., 2010, Jasoni et al., 2005). R_{eco} was measured immediately afterwards and in exactly the same way as the NEE one, except that an opaque cover was placed over the chamber to eliminate light. Midday measurements were made on a total of 88 days over six growing seasons (May through September), and measurement days were typically separated by 2 to 4 weeks. Additional measurements of NEE and R_{eco}, and thus GPP, were made every 6 weeks at five measurement times per day in each plot (nominal times = 04:00, 09:00, 12:00, 16:00 and 21:00). More details on the methods can be found in Bachman *et al.* (2010) and Pendall et al. (2013). See Ryan et al. (2015) for descriptions of the environmental data and the gap-filling employed to estimate missing covariate data on certain days and hours.

Data synthesis and modeling

We fit a non-linear mixed effects model to the GPP data to quantify how GPP varied among the experimental treatments at the season, annual, and multi-annual scales. The goal of this analysis is two-fold: (1) to quantify the combined effects of the categorical treatment effects and the time-varying concurrent and antecedent environmental effects (addressing questions 1 and 2), and (2) to estimate GPP on non-measurements times, while accounting for different sources of uncertainty, thus allowing us to gap-fill the GPP dataset and produce estimates of cumulative GPP fluxes (addressing question 3).

Given the distributional properties of the observed GPP data (GPP^{obs}), we assumed that GPP^{obs} followed a normal distribution. Thus, observation *i* (*i* = 1,…, 2456):

$$GPP_i^{obs} \sim Normal(\mu_i, \sigma_{t(i)}^2) \tag{1}$$

μ is the mean or predicted GPP value, σ^2 represents the observation variance, and *t*(*i*) indicates treatment *t* (*t* = 1, 2, …, 6 treatment levels) associated with observation *i*. We employ a semi-empirical model for the mean GPP, μ, based on the rectangular hyperbola light-response model (Desai et al., 2008, Falge et al., 2001, Thornley, 1976, Landsberg and Waring, 1997), which we adapted to include the effect of atmospheric CO_2 concentration (Acock et al., 1976). We lack sufficient data to parameterize more complex or mechanistic models (E.g. Farquhar et al., 1980). However, the light-response or radiation-use efficiency type model has been frequently applied, in various formulations, to ecosystem level GPP and NPP flux data (see above references), and thus there is good precedence for using it here. The model for μ is:

$$\mu_i = \frac{Q_i PAR_i Amax_i C_i}{Q_i PAR_i + Amax_i C_i} \tag{2}$$

PAR_i is the measured PAR (μmol m^{-2} s^{-1}); Q_i (μmol CO_2 μmol^{-1} quanta) is the quantum yield or canopy light-use efficiency (i.e., the slope of the light response curve at PAR=0); A_{max_i} (μmol C m^{-2} s^{-1}) is the maximum CO_2 uptake rate of the canopy (maximum GPP) at light saturation.

$C_i = c_j \exp\left(CO_{2_i} - \overline{CO_{2_j}}\right)$ accounts for variation in atmospheric CO_2 relative to the mean observed atmospheric [CO_2] ($\overline{CO_{2_j}}$) in the ambient (*j* = 1; ct, cT, ctd, cts) and elevated (*j* = 2; Ct, CT) CO_2 plots, where CO_{2_i} is the measured atmospheric [CO_2], and the parameter c_j describes the effect of deviations from the mean concentration ($\overline{CO_{2_j}}$= 376 ppm and 572 ppm for *j* = 1 and *j* = 2, respectively). An exponential function is applied to the deviations to ensure $C_i > 0$.

To capture potential temporal changes in the GPP response, we modeled Q and A_{max} as functions of various biotic (greenness and N) and abiotic (SWC, Tair, and VPD) factors at both current and antecedent (described in detail in the section below) time-scales. It is well known that plant photosynthesis is partly governed by leaf N content (Williams et al., 1996, Landsberg and Waring, 1997, Magnani et al., 2007) and temperature (Farquhar et al., 1980, Bernacchi et al., 2001) via their effects on enzyme-mediated reactions. VPD also plays an important role via its effect on stomatal conductance, which in turn controls photosynthetic rates (Collatz et al., 1991, Medlyn et al., 2011) . Furthermore, vegetation greenness is expected to correspond to GPP; for example, satellite estimates of GPP are inferred from the light reflectance of the vegetation, which describes greenness of the vegetation. To ensure that A_{max} is positive, we modeled A_{max} on the log scale, and to constrain Q between 0 and 1, we modeled Q on the logit scale. For example, we modeled $\log(A_{max})$ as a linear function of the aforementioned current and antecedent (subscript = ant) biotic and abiotic drivers, with parameters that vary by treatment *t* (*t* = 1, 2, …, 6) associated with observation *i*:

$$\begin{aligned}\log(Amax_i) &= \alpha_{0,t(i)} + \alpha_{1,t(i)}SWC_i + \alpha_{2,t(i)}VPD_i + \alpha_{3,t(i)}Tair_i + \alpha_{4,t(i)}SWC_{ant,i} + \alpha_{5,t(i)}VPD_{ant,i} \\ &+ \alpha_{6,t(i)}Tair_{ant,i} + \alpha_{7,t(i)}N_i + \alpha_{8,t(i)}Greenness_i + \alpha_{9,t(i)}\Delta Greenness_{ant,i} + \text{interactions} + \varepsilon_{t(i),p(t(i))}\end{aligned} \tag{3}$$

$\varepsilon_{t,p}$ represents a plot (nested in treatment) random effect, and *p*(*t*(*i*)) indicates plot *p* associated with treatment *t* and observation *i* (*p* = 1, 2, 3, 4, 5 for each treatment). $\Delta Greenness_{ant}$ represents the antecedent rate of change of greenness; when greenness is increasing, $\Delta Greenness_{ant} > 0$, and when leaves are senescing $\Delta Greenness_{ant} < 0$. We define ‘interactions’ in Eqn (3) to potentially include all 2-way interactions between the covariates indicated in Eqn (3). Preliminary analysis identified five two-way interactions (of 36 possible) that were most important for understanding GPP (see appendix S1 for details of preliminary analysis), including Tair×Tair, SWC_{ant}×$Tair_{ant}$,

SWC_{ant}×VPD_{ant}, SWC×SWC_{ant} Tair×$Tair_{ant}$ and VPD×Tair; these five interactions represent the "interactions" term and are assigned interaction effects parameters $\alpha_{10,t}$ - $\alpha_{15,t}$, respectively. Including these interactions is further justified because: (1) Tair×Tair accounts for a potential peaked temperature response; (2) SWC_{ant}×$Tair_{ant}$ indicates the seasonality of moisture availability; (3) SWC_{ant}×VPD_{ant} indicates differential below- versus aboveground water stress effects; and, (4) previous studies have reported important interactions between current and antecedent factors. Regarding the last point, C fluxes are likely to respond differently to a rain event (increase in current SWC) that occurs during a dry period (low SWC_{ant}) compared to during a wet period (high SWC_{ant}) (Arp, 1991, Barron-Gafford et al., 2014, Cable et al., 2013, Ryan et al., 2015), thus reflecting potential hysteresis patterns (Oikawa et al., 2014, Barron-Gafford et al., 2011).

The function for logit(Q) is the same as for log(A_{max}) except that: (1) there is no N term because N is primarily expected to affect the amount of RuBisCO in the photosynthetic tissues, which in turn primarily limits A_{max} (Reich et al., 2009); and (2) it has its own nested plot random effects and treatment-specific effects parameters (β_0,…, β_{14}) (see Table 3 for a summary of model parameters).

Quantification of antecedent drivers

We characterized and quantified antecedent covariates following the stochastic antecedent modeling (SAM) framework described by Ogle *et al.* (2015); examples of practical implementation are given by Ryan *et al.* (2015), Cable *et al.* (2013), and Barron-Gafford *et al.* (2014). Traditional methods of defining antecedent variables often compute a deterministic average of the variable over a fixed past time period. SAM is different in that it allocates parameters ("importance weights") to specific periods in the past, thus enabling quantification of the relative importance of the variable at those different past times. Following Cable *et al.* (2013) and Ryan *et al*. (2015), we allowed GPP to be influenced by Tair and VPD over daily time-scales, and by SWC and greenness over weekly time-scales. In general, we describe the antecedent variable (X_{ant}) associated with observation *i* as:

$$X_{ant,i} = \sum_{k=1}^{Nperiods} W_{X_{k,t(i)}} \overline{X}_{tp(i)-k+1,p(t(i))} \tag{4}$$

where X = VPD or Tair, $\bar{X}$ is the 24-hour mean for a particular day or time period, *k* is the time lag into the past (for Nperiod = 7 time steps) such that when $k = 1$, $\bar{X}$ is the observed 24-hour mean that occurred during *tp*(*i*), the time period associated with observation *i*; again, *t*(*i*) and *p*(*t*(*i*)) are the treatment ($t = 1,..,6$) and plot (p = 1,..,5 per treatment) associated with observation *i*. W_X are the weight parameters to be estimated. The expression for SWC_{ant} is similar to equation (4) except that $\bar{X}$ is the7-day mean for a particular week such that tp denote the week associated with each observation and *k* denotes the time (week scale) lag (Nperiods = 6); as done in Ryan *et al*. (2015), we allocated a separate weight for each of the first few weeks in the past ($k = 1, 2, 3, 4$), the fifth ($k = 5$) weight to past weeks 5-6, and the sixth ($k = 6$) weight to past weeks 7-10. We made a slight modification to calculate $\Delta Greenness_{ant}$:

$$\Delta Greenness_{ant,i} = \sum_{k=1}^{Nperiods} W_{X_{k,t(i)}} \left(\overline{X}_{tp(i)-k+1,p(t(i))} - \overline{X}_{tp(i)-k,p(t(i))} \right) \tag{5}$$

where $\bar{X}$, *i*, *k*, *t*, *tp*, and *p* are as defined previously for the weekly scale covariates. Like SWC_{ant}, the time periods are on a weekly scale, but $k = 1, 2, 3$, and 4 correspond to the past week, two weeks ago, three weeks ago, and four weeks ago (Nperiods = 4), respectively.

We refer to the model described above as the ‘main’ model. We also implemented an ‘alternative’ model that excludes all antecedent covariates from the Q and A_{max} functions, as defined in Eqn (3), to evaluate the importance of including antecedent effects. The alternative model (no antecedent effects) is more similar to the types of models that are often applied for partitioning eddy-covariance NEE data into its GPP and ecosystem respiration components, such as those described in the review paper by Desai et al. (2008).

Model implementation and assessment

We implemented the model within a hierarchical Bayesian framework (see Appendix S2 for details) using the software package JAGS (Plummer, 2003), which uses Markov chain Monte Carlo (MCMC) to sample from the joint posterior of the model parameters. Depending on the model (main or alternative model), we ran three parallel chains for 100,000-200,000 iterations each. After discarding the first 50% of iterations as 'burn in', we thinned the chains by 100 to reduce within-chain autocorrelation and to reduce storage requirements; convergence was assessed using the Brooks-Gelman-Rubin diagnostic tool (Gelman et al., 2013). This produced roughly 3000 independent samples from the posterior distribution for each parameter, which were summarized by their posterior means, central 95% credible intervals (CIs) defined by the 2.5th and 97.5th percentiles, and Bayesian p-values (Gelman et al., 2013).

We assessed the performance of the model by comparing predicted GPP versus observed GPP. We used the coefficient of determination (R^2) as an informal measure of model accuracy. A limitation with solely using R^2 is that it does not detect when over-fitting occurs, the phenomenon by which R^2 can increase with greater model complexity (more parameters). To overcome this, we also calculated two other commonly used model assessment diagnostics: the deviance information criterion (DIC) and the posterior predictive loss (PPL). Each of these statistics are the sum of a goodness of fit term and a model complexity (penalty) term that describes the effective number of parameters (Spiegelhalter et al., 2002, Gelfand and Ghosh, 1998). One model is more desirable over another if it has a lower DIC and lower PPL. Using these two indices, we compared our main model with the alternative model.

Estimates of seasonal, annual and six-year GPP

Our Bayesian approach to analyzing the GPP data also provides a framework for predicting GPP for time periods for which it was not measured. Each of the fitted models (main and alternative) was subsequently applied on an hourly time-step during the March-October period (we assumed GPP = 0 during other months due to the lack of vegetation during these winter months) for 2007-2012, and for every plot using each of the 3000 parameter sets sampled from the posterior distribution. The model simulations were implemented using equations (2)-(5) as well as all measurements of plot-level data (daily SWC, daily greenness, hourly Tair, hourly VPD, and annual N). The resulting hourly GPP predictions were summed within each season, each year, and across all years for each of the 3000 model executions, yielding posterior predictive distributions of seasonal (spring [March-May], summer [June-August], fall [Sept-Oct]), annual (March-October), and six-year GPP estimates. These distributions account for both model uncertainty (e.g., lack of fit) and parameter uncertainty.

Comparisons to GPP simulated from 12 terrestrial biosphere models

The data-driven predicted GPP values could serve as important 'data-products' for informing and evaluating terrestrial biosphere models (TBMs). Importantly, the Bayesian procedure explicitly quantifies uncertainty in such data products. To exemplify the importance of quantification of data product uncertainty, we considered two different types of data products: (1) six-year cumulative GPP from the main and alternative models as described in the previous subsection, and (2) the percent change in the six-year GPP under warming (cT) and eCO_2 (Ct) relative to the control (ct). As with the first, the second data product was computed using Monte Carlo simulations based on the 3000 posterior estimates of the six-year GPP (see Appendix S3 for description of how both data products were computed). The six-year GPP and GPP responses predicted from 12 TBMs were compared against the corresponding data products. The TBMs included: six land surface models (CABLE, CLM4.0, CLM4.5, ISAM, OCN, and ORCHIDEE); three global dynamic vegetation models (JULES, LPJ-GUESS and SDGVM); and three ecosystem models (DAYCENT, GDAY, and TECO); see Table S1 in the supplementary material for a description of the TBMs. The TBMs were not calibrated to the site using response data, but they were provided optional data or parameter values (e.g., Vcmax, specific leaf area, rooting depth, soil texture) representative of the site. Models were also forced with site meteorological data covering the six years of the experiment (see Appendix S4 for details).

As a result of the TBMs not being rigorously calibrated against the PHACE data, there was no expectation that the TBM responses would match or be close to the expected PHACE responses. The purpose of comparing our "GPP data product" against the TBM output was to illustrate how our data product could be used to inform the TBMs. Our analysis represents a more flexible and potentially more rigorous method for "gap-filling" missing data – compared to algorithms that are currently used to gap fill, for example, fill eddy flux data – and we show how it can be used to generate GPP estimates (data products) over the course of the experiment.

Results

Assessment of model performance

Our main model was able to explain a large portion of the variation in the hourly GPP observations (overall R^2 of 0.79). However, the accuracy of the GPP predictions varied among the treatments (Fig. 1), with treatment-specific fits: cT (R^2=0.86), ctd (R^2=0.81), ct (R^2=0.80), cts

(R^2=0.77), CT (R^2=0.77), and Ct (R^2=0.67). For all treatments, the model tends to slightly under-predict GPP at high values, and while this bias is minimal, it is more pronounced in the Ct treatment (Fig. 1). That is, amongst a number of treatments, there are a handful of measurements that are significantly higher than the modelled values, and these seem to mainly be concentrated on one or two days during the fall (Fig. S5).

The alternative model, which excluded all of the antecedent covariates, resulted in a poorer fit (R^2 = 0.58 overall, R^2 ranged from 0.40 to 0.67 among treatments) and greater bias (more severe under-prediction of GPP at high values) (Fig. S1). The more robust DIC and PPL measures also strongly indicated much better model performance for the main model compared to the alternative model (DIC=12,690 and PPL=45,852 for the main model, with DIC=13,903 and PPL=80,067 for the alternative model).

Phenology of grassland carbon uptake and its relation to precipitation

The time series of predicted GPP revealed high interannual variability (Fig. 2). For example, for the control treatment (ct), predicted daily GPP reached a maximum around 10 g C m^{-2} day^{-1} for 2009 and 2010, which was double the predicted maximum in 2012 (~5 g C m^{-2} day^{-1}; Fig. 2a). Within years, bimodal peaks in GPP were predicted in 2007, 2008, 2011, and 2012 in response to spring and late-summer precipitation inputs.

Treatment effects on GPP

Over the entire experimental period (2007-2012), the largest and most statistically significant increases in GPP relative to the control treatment (ct) occurred under warming (29% increase; Table 1 and Fig. 3b; P=0.02 for ct vs cT), eCO_2 (26%; Table 1 and Fig. 3b; P=0.07 for ct vs Ct), and deep irrigation (28%; Table 1 and Fig. 3b; P<0.01 for ct vs ctd).

At the annual time scale, relative to ct, annual GPP increased under eCO_2 (Ct) in 2007, 2008, 2011, and 2012 (Fig. 3a and Table 1; ct vs Ct, P=0.007, 0.09, 0.02 and 0.009, respectively). Warming (cT) also stimulated annual GPP in 2007, 2008, 2010, and 2011 (Fig. 3a and Table 1; ct vs cT, P=0.006, 0.04, 0.09, and 0.005 respectively). There is some evidence that the combination of eCO_2 and warming (CT) enhanced GPP in 2007 and 2011 (Fig. 3a and Table 1; ct vs CT, P=0.09 and 0.08, respectively). The large increase in GPP under deep irrigation (ctd) was reflected across individual years, with four showing statistically significant increases of 28-61%. In the absence of warming, annual GPP under eCO_2 (Ct) was similar to annual GPP under shallow irrigation (cts) for all years (Table 1; Ct vs cts, P>0.18 for any individual year).

Seasonal differences in the treatment effects emerged. The 29% overall increase in GPP under warming (cT) relative to the control (ct) during all six years was primarily driven by enhanced spring productivity (Fig. 3b, black-filled portion of cT bars; Table 1, ct vs cT: 129% increase, P=0.001). During the summer, there was on average an 11% decline in GPP under cT (Table 1, ct vs cT, P=0.15), which is consistent with Pendall *et al.* (2013) who used linear regression and linear interpolation to estimate April-September GPP sums from data. Although the CO_2 effect was only statistically significant (P<0.09) for four out of the six years, GPP increased by 124% under eCO_2 (Ct) during fall. The spring cT and fall Ct GPP estimates were the only treatment by season combinations that were always significantly different (P<0.03) from the corresponding season-level ct estimates, for all years (Table 2, rows 1 and 3). Compared to spring and summer, GPP also increased the most during fall under eCO_2 and warming (ct vs CT: 42% increase, P=0.03), deep irrigation (ct vs ctd: 68% increase, P=0.002), and shallow irrigation (ct vs cts: 66% increase, P=0.008) (Table 1).

Importance of current and antecedent conditions for understanding treatment effects on GPP

Including antecedent terms in the submodels for A_{max} and Q (see Eqn (3)) resulted in decreases in the predicted six-year GPP relative to the alternative model, with the greatest reductions occurring for the control treatment (by 12%, P=0.14), the eCO_2 × warming treatment (by 20%, P=0.04), and the deep irrigation treatment (by 14%, P=0.05). Furthermore, 34 out of the 36 treatment × year combinations corresponded to a decrease in annual GPP of between 1% and 42% for the main model versus the alternative model (Tables S3a, S3b, S3c). Both A_{max} and Q were not significantly affected by concurrent covariates (SWC, VPD, Tair, greenness, and N), for most or all treatments, depending on the covariate (Table 3). Conversely, the main effect of two of the three antecedent covariates (VPD_{ant} and $Tair_{ant}$) on A_{max} was significant for the majority of treatments (Fig. 4a,b; Table 3). The most important predictors for Q involved the SWC_{ant}×$Tair_{ant}$ and SWC_{ant}×VPD_{ant} interactions, which were significant for four and three of the treatments, respectively (Fig. 4c,d; Table 3). Although the direction of the VPD_{ant} (for A_{max}), $Tair_{ant}$ (A_{max}), SWC_{ant}×$Tair_{ant}$ (Q), and SWC_{ant}×VPD_{ant} (Q) effects were consistent for the vast majority of treatments (Table 3), the magnitude of the antecedent effects differed among certain pairs of treatments (Fig. 4a,c,d).

Given that antecedent conditions are important for understanding GPP, we can evaluate the time-scales over which each variable influences GPP. For SWC_{ant}, the first two weeks prior to the GPP measurement were generally the most important for predicting GPP (Fig. S2a). For the majority of treatments, Tair experienced 3-4 days prior and VPD from 1-3 days prior tended to be the most important for predicting GPP (Fig. S2b,c).

Comparison of predicted six-year GPP with TBMs

When comparing the GPP predictions from our data-driven analysis with those of 12 terrestrial biosphere models (TBMs), the 95% credible intervals (CIs) of our six-year GPP "data product" (whether generated from the main or alternative model) under the control (ct) and eCO_2 (Ct) treatments are fairly narrow compared to the range of TBM predictions (Fig. 5a,b). Under the control treatment, only one of the twelve TBM predictions fell within the 95% CI of the data product if antecedent conditions were included in the calculation of the data product (Fig. 5a, black cross and error bar). The number of TBM predictions consistent, or almost so, with the data product increased to five if antecedent conditions were not included when computing the data product (Fig. 5a, grey cross and error bar). Under the eCO_2 scenario, there was greater similarity in the number of TBM predictions agreeing with the data product if antecedent versus no antecedent conditions were included for determining the data product (Fig. 5b).

The TBMs also need to accurately predict the relative change in GPP under scenarios of environmental change (e.g., eCO_2, warming, or some combination). We used our GPP analysis framework to produce a data product of the percent difference in GPP under treatment conditions relative to control conditions. In contrast to the cumulative GPP estimates, these percent differences were associated with high uncertainty, sometimes spanning both decreases and increases (e.g., Fig. 5c,d). This resulted in the majority of TBM simulations that are consistent with this data product (i.e., the TBM predictions lie within the CIs; Fig. 5c,d), despite the wide range of TBM predictions. Thus, the data product associated with GPP on the absolute scale (Figs. 3a,b) is more useful for evaluating and informing TBMs than the data product on the percent change scale (e.g. Figs. 3c,d).

Discussion

Implications of treatment effects on annual GPP

Annual GPP was predicted to be most stimulated by elevated CO_2 (eCO_2, Ct treatment) during the three driest years of our study (2007, 2011, and 2012), suggesting that increased GPP under eCO_2 could have resulted from enhanced water-use efficiency (Kelly et al., 2015). The shallow irrigation (cts) treatment confirmed the role of SWC in mediating the GPP responses to eCO_2, consistent with findings in a similar grassland system (Parton et al., 2012). Moreover, deep irrigation led to a greater percentage increase in GPP compared with eCO_2 or surface irrigation (Table 1; Fig. 3). This may reflect the frequency and magnitude in which irrigation was applied under ctd (twice, large events) compared to cts (three-five smaller events). Larger, less frequent precipitation events are expected to stimulate GPP to a greater extent than smaller, more frequent events, especially early in the growing season (Heisler-White et al., 2008, Lauenroth and Sala, 1992, Ogle et al., 2015). A prior estimate of annual GPP for this same site suggested a reduction in GPP by eCO_2 in 2009 (Pendall et al., 2013), but our analysis revealed that a significant difference existed only during summer of that year (P=0.06). We also found that 2009 – the wettest year – had the highest annual GPP under the control treatment compared to all other study years(Fig. 3, Table S2, Table S3a), in agreement with Mueller et al. (2016) who found the highest aboveground biomass in that year but no eCO_2 effect. Other grassland studies have found no response or a reduction in primary production under eCO_2 during wet years (Hovenden et al., 2014, Polley et al., 2013).

Climate change treatments altered the seasonality of GPP, particularly in spring and fall, as observed for species and community-level measurements at the same site (Reyes-Fox et al., 2014, Zelikova et al., 2015). Across all years, warming (cT) consistently increased annual GPP by 12-50%, and this was predominantly driven by enhanced production during the spring (Fig. 3a; Tables 1,2), when temperature limits constrained productivity in this high elevation system. Increased annual GPP for all treatments, except cT, relative to the control (ct) was dominated by increases in GPP during the fall (Table 1, furthest right column). The consistency of the statistical significance of this eCO_2 enhancement during fall of most years, as well as the warming enhancement in spring (Table 2), may be due to two potential co-occurring mechanisms: (i) Spring warming directly stimulates earlier snow melt, photosynthesis, and plant growth (Figs. S4, Luo, 2007, Richardson et al., 2010b, Sherry et al., 2008); and/or (ii) the SWC in fall is sustained for longer as a result of the water-saving effects of eCO_2 in water limited systems like at PHACE (Webb et al., 2012, Morgan et al., 2004, Morgan et al., 2011, Nowak et al., 2004). Our results indicate that these GPP enhancements in spring and fall may extend the growing season. For example, in 2008 (an average year in terms of meteorology), modelled GPP during spring was consistently higher under warming, although observed GPP showed only a minor increase (Fig. S5a and S5c). In fall, modelled GPP remained significantly higher with eCO_2 compared to ambient, which is supported by the observations (Fig S5b,d). In the warm, dry year of 2012, GPP was significantly enhanced by warming in spring and by eCO_2 in fall (Table 3). This is partly consistent with observed treatment effects on vegetation greenness (Zelikova et al., 2015), which was stimulated by the combination of warming and eCO_2 in spring of 2012. Overall, our data-model product provides reasonable support for hypothesized mechanisms that could extend the growing season in this cool, dry grassland, although additional observations in spring and fall could improve confidence in climate change effects on ecosystem physiology (Richardson et al., 2010a, Richardson et al., 2013).

Importance of antecedent conditions for predicting GPP and evaluating treatment differences

An increasing number of studies recognize the importance of antecedent conditions in understanding the terrestrial C cycle (Barron-Gafford et al., 2014, Cable et al., 2013, Ryan et al., 2015, Gamnitzer et al., 2011). Our main model (with antecedent effects) explained 67-86% of the variation in the GPP data, but the alternative model (without antecedent effects) only explained 40-67% of the variation. This difference in the explanatory power of models that include antecedent conditions has also been demonstrated for other C flux components, including soil respiration (Ogle et al., 2015, Barron-Gafford et al., 2014), annual aboveground NPP, and annual tree growth (Ogle et al., 2015). The increased explanatory power of the “antecedent models” cannot not be solely explained by the additional parameters that they introduce given the support conveyed by model selection indices that penalize for the number of parameters or model complexity. In particular, our results suggest that antecedent vapor pressure deficit (VPD_{ant}) and antecedent air temperature ($Tair_{ant}$) were the most important predictors of GPP, primarily via their effects on maximum potential GPP (A_{max}). Antecedent SWC (SWC_{ant}) interacted with these two factors to affect light-use efficiency (Q).

The importance of $Tair_{ant}$ suggests that accounting for seasonal changes in air temperature is critical for obtaining good estimations of A_{max} in this temperate grassland, especially in spring when moisture is less limiting (Lauenroth and Sala, 1992). The importance of antecedent temperature has been implicated as depicting a temperature acclimation response (Ogle et al., 2015). However, the general positive effect of $Tair_{ant}$ on A_{max} actually indicates that warmer past temperatures tend to enhance A_{max} and GPP, regardless of the current air temperature which appears to have little impact on GPP once antecedent temperature is accounted for (see Table 3). It appears that GPP is more likely to respond to concurrent changes in soil water (SWC), and to some extent VPD, compared to temperature. The importance of concurrent SWC and VPD on GPP likely reflects stomatal regulation of plant water status, which in turn is expected to affect photosynthesis, and thus GPP.

While we would expect GPP to be partly regulated by short-term (sub-daily) changes in VPD (e.g., via stomatal control; Oren et al. 1999), we also found that VPD experienced over the past few days (VPD_{ant}) affects GPP, especially through its influence on A_{max}. In particular, high VPD for about 1-3 days prior, is predicted to reduce A_{max}, across all treatments (Fig. 4a). While the effect of VPD on stomatal closure and photosynthesis is usually treated as being instantaneous due to tight coupling of stomatal conductance to VPD (Collatz et al., 1991), this study suggests that plants may adjust to VPD over longer time scales. VPD conditions occurring over the past 1-7 days represent a proxy for past atmospheric drought conditions (Haddad et al., 2002), and GPP is likely to be negatively impacted by cumulative atmospheric drought. Furthermore, the VPD_{ant} effect was more negative under eCO_2 (Fig. 4a), indicating greater sensitivity of stomata (and hence, photosynthesis) to atmospheric drought, potentially leading to higher integrated water-use efficiency under eCO_2.

The use of VPD as a predictor of GPP is not new (Groenendijk et al., 2011), but the proposition that antecedent VPD is an important driver of GPP has not been previously considered. One possibility is that this effect is just an artifact of our model because VPD depends upon Tair, and the VPD_{ant} effect could reflect a non-linear $Tair_{ant}$ effect. However, this is unlikely because although current VPD is highly correlated with current Tair ($r = 0.85$), the correlation between the antecedent covariates (VPD_{ant} versus $Tair_{ant}$) is weaker ($r = 0.68$). Furthermore, our model contains quadratic Tair ($Tair^2$) terms in both the A_{max} and Q functions, thus the shape of the expected response of GPP to Tair (peaked) should already be accounted for. A more plausible explanation for the VPD_{ant} effect is that stomatal conductance or photosynthesis acclimate to VPD. For example, Kutsch et al. (2001) found that a decrease in stomatal aperture in beech trees – implying a decrease in GPP – was negatively correlated with the previous month's mean VPD. The importance of past VPD, rather than past SWC, prompted the authors to suggest that plants possess a biochemical memory of past climatic conditions. Buckley (2005) further suggests that when VPD exceeds some threshold, water potential can reach a cavitation threshold, leading to cavitation and reducing transpiration at any given VPD. If VPD is subsequently reduced, then there is a lag between the recovery of water potential and embolism repair; the time scale of this recovery is not well understood but could contribute to a GPP versus VPD lag. Various mechanisms have been proposed to explain the stomatal behavior versus VPD lag including the hydroactive feedback hypothesis (Buckley 2016) or delays associated with abscisic-acid (ABA) signalling (Aliniaeifard and van Meeteren, 2014). Clearly, additional research is required to establish the generality of a GPP versus VPD lag (antecedent effect) and to identify underlying mechanisms related to stomatal behavior, biochemical acclimation, or other explanations.

Terrestrial biosphere models (TBMs) do not commonly account for the potential direct effects of antecedent VPD on the physiological components, for example, through acclimation of photosynthesis (Kattge and Knorr, 2007, Smith et al., 2015). Nevertheless, soil water content does contain information on antecedent VPD, and thus via soil water effects on physiology models have an indirect "memory" of VPD. However, model physiological responses to changes in soil water are empirical and can range from insensitive to too sensitive (De Kauwe et al., 2015, De Kauwe et al., 2014). First principles methods that integrate carbon costs and benefits under antecedent environmental conditions (De Kauwe et al., in review, Mueller et al., 2016) may provide a robust method to incorporate acclimation of leaf physiology to antecedent VPD and soil water into TBMs. Our results highlight accounting for such an acclimation process, which directly considers the effect of antecedent conditions, could improve modelled estimates of photosynthesis.

Implications for the terrestrial carbon cycle

Estimates of global GPP used in the last IPCC report were calculated from site-level GPP estimates that were derived by fitting a light response curve to flux tower NEE data (Beer et al., 2010, Lasslop et al., 2010). The site-level A_{max} terms in these analyses were also represented as exponential functions of current environmental covariates (Lasslop et al., 2010). If antecedent conditions (such as VPD_{ant}, SWC_{ant}, and $Tair_{ant}$) had been included, our analysis suggests that annual estimates of GPP at semi-arid grasslands could have been improved (Fig. 1 vs. Fig. S1). For other ecosystems or plant functional types that are less sensitive to drought, the effect of antecedent meteorological conditions may be less pronounced. Moreover, our results show that including antecedent conditions could result in lower estimates of cumulative GPP in temperate grasslands under current climate (by 12%), and especially under a future, warmer climate and eCO_2 (by 20%; see Table S3c).

Since the early 1990s, global change experiments, such as Free Air CO_2 Enrichment (FACE) studies, have generated data on responses of key biogeochemical processes to future environmental conditions. Such experiments have become invaluable for informing model forecasts (Piao et al., 2013, Zaehle et al., 2014, De Kauwe et al., 2014, Walker et al., 2014, De Kauwe et al., in review). One of the challenges associated with applying terrestrial biosphere models (TBMs) to understand climate change impacts on GPP and the C cycle is limited access to accurate data products for informing and evaluating the models. Since many data products are derived from simpler models that are fit to observational data, it is prudent to account for uncertainty in such data products since they are not perfect representations of the real system.

Our hierarchical Bayesian approach to analyzing the GPP data in the context of a fairly simple light-response model provides a mechanism for predicting GPP at non-measurement time-periods, while accounting for uncertainty in these predictions. However, we wish to emphasize that the purpose of the comparison between TBMs and our "data product" (Fig. 5) was not to validate the TBMs, but rather to evaluate the utility of the data products.

We are confident in our seasonal, annual, and six-year cumulative GPP predictions given their relatively narrow 95% CIs (e.g., Fig. 5a and 3b). The width of the intervals, however, did vary among global change treatments, with the widest intervals (and weakest model fits [lowest R^2s]) occurring for treatments involving eCO_2 (Ct and CT). This suggests that additional information or improved model structure is required to obtain more accurate GPP estimates under eCO_2. In general, the tight estimates for cumulative GPP at different time scales suggest that this would be a valuable (semi-)independent data stream that TBMs can be compared against.

The importance of antecedent environmental conditions on grassland GPP has been highlighted by the Bayesian model selection procedure used in this study. Antecedent conditions were key predictors of GPP, in particular air temperature and vapor pressure deficit of the past week, and research into the mechanism by which antecedent Tair and VPD affect GPP would be an interesting and useful contribution to understanding the carbon cycle in these grassland ecosystems. Including antecedent conditions substantially improved the fit of the Bayesian model and led to a consistent reduction in the computed multi-year GPP in this grassland ecosystem, across the vast majority of treatments and years. Given the global coverage of grassland ecosystems, understanding the effect of antecedent environmental conditions more broadly is likely to have implications for our understanding of the global carbon cycle.

Data availability

Data are available through the digital repository, Dryad. Please e-mail Elise Pendall (E.Pendall@westernsydney.edu.au) or Edmund Ryan (edmund.ryan@lancaster.ac.uk) for details.

Acknowledgements

This material is based upon work supported by the US Department of Agriculture, Agricultural Research Service Climate Change, Soils & Emissions Program, USDA-CSREES Soil Processes Program (#2008-35107-18655), US Department of Energy Office of Science (BER), through the Terrestrial Ecosystem Science program (#DE-SC0006973) and the Western Regional Center of the National Institute for Climatic Change Research, and by the National Science Foundation (DEB#1021559). Any opinions, findings, and conclusions or recommendations expressed in this material are those of the author(s) and do not necessarily reflect the views of the National Science Foundation. We thank D. LeCain, J.A. Morgan, J. Heisler-White, A. Brennan, S. Bachman, Y. Sorokin, T.J. Zelikova, D. Blumenthal, K. Mueller and numerous others for assistance in data collection and operation of PHACE facilities, and B. Yang for use of his gap-filled meteorological data at the site. We also thank D. Kinsman for his helpful comments on the discussion section.

Author contributions

ER, KO, and EP designed the study; ER conducted the analysis and wrote the paper, with contributions from KO, EP, AW, MDK, and BM. The Bayesian analysis was directed by KO; DP assisted with implementing the Bayesian models. The remaining authors provided GPP model output from eight of the TBMs in order to construct Figure 5.

References

ACOCK, B., HAND, D., THORNLEY, J. & WILSON, J. W. 1976. Photosynthesis in stands of green peppers. An application of empirical and mechanistic models to controlled-environment data. *Annals of Botany,* 40**,** 1293-1307.

AINSWORTH, E. A. & LONG, S. P. 2005. What have we learned from 15 years of free-air CO2 enrichment (FACE)? A meta-analytic review of the responses of photosynthesis, canopy properties and plant production to rising CO2. *New Phytologist,* 165**,** 351-372.

ALINIAEIFARD, S. & VAN MEETEREN, U. 2014. Natural variation in stomatal response to closing stimuli among Arabidopsis thaliana accessions after exposure to low VPD as a tool to recognize the mechanism of disturbed stomatal functioning. *Journal of experimental botany,* 65**,** 6529-6542.

ARORA, V. K., BOER, G. J., FRIEDLINGSTEIN, P., EBY, M., JONES, C. D., CHRISTIAN, J. R., BONAN, G., BOPP, L., BROVKIN, V. & CADULE, P. 2013. Carbon–concentration and carbon–climate feedbacks in CMIP5 Earth system models. *Journal of Climate,* 26**,** 5289-5314.

ARP, W. 1991. Effects of source-sink relations on photosynthetic acclimation to elevated CO2. *Plant, Cell & Environment,* 14**,** 869-875.

BACHMAN, S., HEISLER-WHITE, J. L., PENDALL, E., WILLIAMS, D. G., MORGAN, J. A. & NEWCOMB, J. 2010. Elevated carbon dioxide alters impacts of precipitation pulses on ecosystem photosynthesis and respiration in a semi-arid grassland. *Oecologia,* 162**,** 791-802.

BARRON-GAFFORD, G. A., CABLE, J. M., BENTLEY, L. P., SCOTT, R. L., HUXMAN, T. E., JENERETTE, G. D. & OGLE, K. 2014. Quantifying the timescales over which exogenous and endogenous conditions affect soil respiration. *New Phytologist,* 202**,** 442-454.

BARRON-GAFFORD, G. A., SCOTT, R. L., JENERETTE, G. D. & HUXMAN, T. E. 2011. The relative controls of temperature, soil moisture, and plant functional group on soil CO2 efflux at diel, seasonal, and annual scales. *Journal of Geophysical Research: Biogeosciences (2005–2012),* 116.

BEER, C., REICHSTEIN, M., TOMELLERI, E., CIAIS, P., JUNG, M., CARVALHAIS, N., RÖDENBECK, C., ARAIN, M. A., BALDOCCHI, D. & BONAN, G. B. 2010. Terrestrial gross carbon dioxide uptake: global distribution and covariation with climate. *Science,* 329**,** 834-838.

BERNACCHI, C., SINGSAAS, E., PIMENTEL, C., PORTIS JR, A. & LONG, S. 2001. Improved temperature response functions for models of Rubisco-limited photosynthesis. *Plant, Cell & Environment,* 24**,** 253-259.

BUCKLEY, T. N. 2005. The control of stomata by water balance. *New Phytologist,* 168**,** 275-291.

CABLE, J. M., OGLE, K., BARRON-GAFFORD, G. A., BENTLEY, L. P., CABLE, W. L., SCOTT, R. L., WILLIAMS, D. G. & HUXMAN, T. E. 2013. Antecedent conditions influence soil respiration differences in shrub and grass patches. *Ecosystems,* 16**,** 1230-1247.

CARRILLO, Y., DIJKSTRA, F. A., LECAIN, D., MORGAN, J. A., BLUMENTHAL, D., WALDRON, S. & PENDALL, E. 2014. Disentangling root responses to climate change in a semiarid grassland. *Oecologia***,** 1-13.

CHAPIN III, F. S., WOODWELL, G. M., RANDERSON, J. T., RASTETTER, E. B., LOVETT, G. M., BALDOCCHI, D. D., CLARK, D. A., HARMON, M. E., SCHIMEL, D. S. & VALENTINI, R. 2006. Reconciling carbon-cycle concepts, terminology, and methods. *Ecosystems,* 9**,** 1041-1050.

CIAIS, P., SABINE, C., BALA, G., BOPP, L., BROVKIN, V., CANADELL, J., CHHABRA, A., DEFRIES, R., GALLOWAY, J. & HEIMANN, M. 2014. Carbon and other biogeochemical cycles. *Climate Change 2013: The Physical Science Basis. Contribution of Working Group I to the Fifth Assessment Report of the Intergovernmental Panel on Climate Change.* Cambridge University Press.

COLLATZ, G. J., BALL, J. T., GRIVET, C. & BERRY, J. A. 1991. Physiological and environmental regulation of stomatal conductance, photosynthesis and transpiration: a model that includes a laminar boundary layer. *agricultural and forest meteorology,* 54**,** 107-136.

COLLINS, M., KNUTTI, R., ARBLASTER, J., DUFRESNE, J.-L., FICHEFET, T., FRIEDLINGSTEIN, P., GAO, X., GUTOWSKI, W., JOHNS, T. & KRINNER, G. 2013. Long-term climate change: projections, commitments and irreversibility.

COX, P. M., BETTS, R. A., JONES, C. D., SPALL, S. A. & TOTTERDELL, I. J. 2000. Acceleration of global warming due to carbon-cycle feedbacks in a coupled climate model. *Nature,* 408**,** 184-187.

DE KAUWE, M., MEDLYN, B. E., WALKER, A. P., ZAEHLE, S., ASAO, S., GUENET, B., HARPER, A., HICKLER, T., JAIN, A., LUO, Y., LU, C., LUUS, K., PARTON, W. J., SHU, S., WANG, Y., WERNER, C., XIA, J., PENDALL, E., MORGAN, J. A., RYAN, E. M., CARRILLO, Y., DIJKSTRA, F. A. & NORBY, R. J. in review. Challenging terrestrial biosphere models with data from the long-term multi-factor Prairie Heating and CO2 Enrichment experiment. *Global Change Biology*.

DE KAUWE, M., ZHOU, S.-X., MEDLYN, B., PITMAN, A., WANG, Y.-P., DUURSMA, R. & PRENTICE, I. 2015. Do land surface models need to include differential plant species responses to drought? Examining model predictions across a latitudinal gradient in Europe. *Biogeosciences Discussions,* 12.

DE KAUWE, M. G., MEDLYN, B. E., ZAEHLE, S., WALKER, A. P., DIETZE, M. C., WANG, Y. P., LUO, Y., JAIN, A. K., EL-MASRI, B. & HICKLER, T. 2014. Where does the carbon go? A model–data intercomparison of vegetation carbon allocation and turnover processes at two temperate forest free-air CO2 enrichment sites. *New phytologist,* 203**,** 883-899.

DESAI, A. R., RICHARDSON, A. D., MOFFAT, A. M., KATTGE, J., HOLLINGER, D. Y., BARR, A., FALGE, E., NOORMETS, A., PAPALE, D. & REICHSTEIN, M. 2008. Cross-site evaluation of eddy covariance GPP and RE decomposition techniques. *Agricultural and forest meteorology,* 148**,** 821-838.

DIELEMAN, W. I., VICCA, S., DIJKSTRA, F. A., HAGEDORN, F., HOVENDEN, M. J., LARSEN, K. S., MORGAN, J. A., VOLDER, A., BEIER, C. & DUKES, J. S. 2012. Simple additive effects are rare: a quantitative review of plant biomass and soil process responses to combined manipulations of CO2 and temperature. *Global Change Biology,* 18**,** 2681-2693.

DUKES, J. S., CHIARIELLO, N. R., CLELAND, E. E., MOORE, L. A., SHAW, M. R., THAYER, S., TOBECK, T., MOONEY, H. A. & FIELD, C. B. 2005. Responses of

grassland production to single and multiple global environmental changes. *PLoS biology,* 3**,** e319.
FALGE, E., BALDOCCHI, D., OLSON, R., ANTHONI, P., AUBINET, M., BERNHOFER, C., BURBA, G., CEULEMANS, R., CLEMENT, R. & DOLMAN, H. 2001. Gap filling strategies for defensible annual sums of net ecosystem exchange. *Agricultural and forest meteorology,* 107**,** 43-69.
FARQUHAR, G., VON CAEMMERER, S. V. & BERRY, J. 1980. A biochemical model of photosynthetic CO2 assimilation in leaves of C3 species. *Planta,* 149**,** 78-90.
FAY, P. A., CARLISLE, J. D., KNAPP, A. K., BLAIR, J. M. & COLLINS, S. L. 2003. Productivity responses to altered rainfall patterns in a C4-dominated grassland. *Oecologia,* 137**,** 245-251.
FRIEDLINGSTEIN, P., COX, P., BETTS, R., BOPP, L., VON BLOH, W., BROVKIN, V., CADULE, P., DONEY, S., EBY, M. & FUNG, I. 2006. Climate-carbon cycle feedback analysis: Results from the C4MIP model intercomparison. *Journal of Climate,* 19**,** 3337-3353.
FRIEDLINGSTEIN, P., MEINSHAUSEN, M., ARORA, V. K., JONES, C. D., ANAV, A., LIDDICOAT, S. K. & KNUTTI, R. 2014. Uncertainties in CMIP5 climate projections due to carbon cycle feedbacks. *Journal of Climate,* 27**,** 511-526.
GAMNITZER, U., MOYES, A., BOWLING, D. & SCHNYDER, H. 2011. Measuring and modelling the isotopic composition of soil respiration: insights from a grassland tracer experiment. *Biogeosciences,* 8**,** 1333-1350.
GELFAND, A. E. & GHOSH, S. K. 1998. Model choice: A minimum posterior predictive loss approach. *Biometrika,* 85**,** 1-11.
GELMAN, A., CARLIN, J. B., STERN, H. S., DUNSON, D. B., VEHTARI, A. & RUBIN, D. B. 2013. *Bayesian data analysis*, CRC press.
GROENENDIJK, M., DOLMAN, A., AMMANN, C., ARNETH, A., CESCATTI, A., DRAGONI, D., GASH, J., GIANELLE, D., GIOLI, B. & KIELY, G. 2011. Seasonal variation of photosynthetic model parameters and leaf area index from global Fluxnet eddy covariance data. *Journal of Geophysical Research: Biogeosciences (2005–2012),* 116.
HADDAD, N. M., TILMAN, D. & KNOPS, J. M. 2002. Long-term oscillations in grassland productivity induced by drought. *Ecology letters,* 5**,** 110-120.
HEISLER-WHITE, J. L., KNAPP, A. K. & KELLY, E. F. 2008. Increasing precipitation event size increases aboveground net primary productivity in a semi-arid grassland. *Oecologia,* 158**,** 129-140.
HOVENDEN, M. J., NEWTON, P. C. & WILLS, K. E. 2014. Seasonal not annual rainfall determines grassland biomass response to carbon dioxide. *Nature,* 511**,** 583-586.
HUXMAN, T. E., SNYDER, K. A., TISSUE, D., LEFFLER, A. J., OGLE, K., POCKMAN, W. T., SANDQUIST, D. R., POTTS, D. L. & SCHWINNING, S. 2004. Precipitation pulses and carbon fluxes in semiarid and arid ecosystems. *Oecologia,* 141**,** 254-268.
JASONI, R. L., SMITH, S. D. & ARNONE, J. A. 2005. Net ecosystem CO2 exchange in Mojave Desert shrublands during the eighth year of exposure to elevated CO2. *Global Change Biology,* 11**,** 749-756.
KATTGE, J. & KNORR, W. 2007. Temperature acclimation in a biochemical model of photosynthesis: a reanalysis of data from 36 species. *Plant, Cell & Environment,* 30**,** 1176-1190.

KELLY, J. W., DUURSMA, R. A., ATWELL, B. J., TISSUE, D. T. & MEDLYN, B. E. 2015. Drought× CO2 interactions in trees: a test of the low-intercellular CO2 concentration (Ci) mechanism. *New Phytologist*.

KIMBALL, B. 2005. Theory and performance of an infrared heater for ecosystem warming. *Global Change Biology,* 11**,** 2041-2056.

KNAPP, A. K. & SMITH, M. D. 2001. Variation among biomes in temporal dynamics of aboveground primary production. *Science,* 291**,** 481-484.

KUTSCH, W. L., HERBST, M., VANSELOW, R., HUMMELSHOJ, P., JENSEN, N. O. & KAPPEN, L. 2001. Stomatal acclimation influences water and carbon fluxes of a beech canopy in northern Germany. *Basic and Applied Ecology,* 2**,** 265-281.

LANDSBERG, J. & WARING, R. 1997. A generalised model of forest productivity using simplified concepts of radiation-use efficiency, carbon balance and partitioning. *Forest Ecology and Management,* 95**,** 209-228.

LASSLOP, G., REICHSTEIN, M., PAPALE, D., RICHARDSON, A. D., ARNETH, A., BARR, A., STOY, P. & WOHLFAHRT, G. 2010. Separation of net ecosystem exchange into assimilation and respiration using a light response curve approach: critical issues and global evaluation. *Global Change Biology,* 16**,** 187-208.

LAUENROTH, W. & SALA, O. E. 1992. Long-term forage production of North American shortgrass steppe. *Ecological Applications,* 2**,** 397-403.

LUO, Y. 2007. Terrestrial carbon-cycle feedback to climate warming. *Annu. Rev. Ecol. Evol. Syst.,* 38**,** 683-712.

LUO, Y., GERTEN, D., LE MAIRE, G., PARTON, W. J., WENG, E., ZHOU, X., KEOUGH, C., BEIER, C., CIAIS, P. & CRAMER, W. 2008. Modeled interactive effects of precipitation, temperature, and [CO2] on ecosystem carbon and water dynamics in different climatic zones. *Global Change Biology,* 14**,** 1986-1999.

LUO, Y., HUI, D. & ZHANG, D. 2006. Elevated CO2 stimulates net accumulations of carbon and nitrogen in land ecosystems: a meta-analysis. *Ecology,* 87**,** 53-63.

MAGNANI, F., MENCUCCINI, M., BORGHETTI, M., BERBIGIER, P., BERNINGER, F., DELZON, S., GRELLE, A., HARI, P., JARVIS, P. G. & KOLARI, P. 2007. The human footprint in the carbon cycle of temperate and boreal forests. *Nature,* 447**,** 849-851.

MCLEOD, A. & LONG, S. 1999. Free-air carbon dioxide enrichment (FACE) in global change research: a review. *Advances in ecological research,* 28**,** 1-56.

MEDLYN, B. E., DUURSMA, R. A., EAMUS, D., ELLSWORTH, D. S., PRENTICE, I. C., BARTON, C. V., CROUS, K. Y., DE ANGELIS, P., FREEMAN, M. & WINGATE, L. 2011. Reconciling the optimal and empirical approaches to modelling stomatal conductance. *Global Change Biology,* 17**,** 2134-2144.

MIGLIETTA, F., HOOSBEEK, M., FOOT, J., GIGON, F., HASSINEN, A., HEIJMANS, M., PERESSOTTI, A., SAARINEN, T., VAN BREEMEN, N. & WALLEN, B. 2001. Spatial and temporal performance of the MiniFACE (Free Air CO2 Enrichment) system on bog ecosystems in northern and central Europe. *Environmental Monitoring and Assessment,* 66**,** 107-127.

MORGAN, J., PATAKI, D. E., KÖRNER, C., CLARK, H., DEL GROSSO, S., GRÜNZWEIG, J., KNAPP, A., MOSIER, A., NEWTON, P. & NIKLAUS, P. A. 2004. Water relations in grassland and desert ecosystems exposed to elevated atmospheric CO2. *Oecologia,* 140**,** 11-25.

MORGAN, J. A., LECAIN, D. R., MOSIER, A. R. & MILCHUNAS, D. G. 2001. Elevated CO2 enhances water relations and productivity and affects gas exchange in C3 and C4 grasses of the Colorado shortgrass steppe. *Global Change Biology,* 7**,** 451-466.
MORGAN, J. A., LECAIN, D. R., PENDALL, E., BLUMENTHAL, D. M., KIMBALL, B. A., CARRILLO, Y., WILLIAMS, D. G., HEISLER-WHITE, J., DIJKSTRA, F. A. & WEST, M. 2011. C4 grasses prosper as carbon dioxide eliminates desiccation in warmed semi-arid grassland. *Nature,* 476**,** 202-205.
MUELLER, K., BLUMENTHAL, D. M., PENDALL, E., CARRILLO, Y., DIJKSTRA, F., WILLIAMS, D., FOLLETT, R. & MORGAN, J. 2016. Impacts of warming and elevated CO2 on a semi-arid grassland are non-additive, shift with precipitation, and reverse over time. *Ecology Letters,* 19**,** 956-966.
NORBY, R. J. & LUO, Y. 2004. Evaluating ecosystem responses to rising atmospheric CO2 and global warming in a multi-factor world. *New Phytologist,* 162**,** 281-293.
NORBY, R. J. & ZAK, D. R. 2011. Ecological lessons from free-air CO2 enrichment (FACE) experiments. *Annual review of ecology, evolution, and systematics,* 42**,** 181.
NOWAK, R. S., ELLSWORTH, D. S. & SMITH, S. D. 2004. Functional responses of plants to elevated atmospheric CO2–do photosynthetic and productivity data from FACE experiments support early predictions? *New phytologist,* 162**,** 253-280.
OGLE, K., BARBER, J. J., BARRON-GAFFORD, G. A., BENTLEY, L. P., YOUNG, J. M., HUXMAN, T. E., LOIK, M. E. & TISSUE, D. T. 2015. Quantifying ecological memory in plant and ecosystem processes. *Ecology letters,* 18**,** 221-235.
OIKAWA, P., GRANTZ, D., CHATTERJEE, A., EBERWEIN, J., ALLSMAN, L. & JENERETTE, G. 2014. Unifying soil respiration pulses, inhibition, and temperature hysteresis through dynamics of labile soil carbon and O2. *Journal of Geophysical Research: Biogeosciences,* 119**,** 521-536.
PARTON, W., MORGAN, J., SMITH, D., DEL GROSSO, S., PRIHODKO, L., LECAIN, D., KELLY, R. & LUTZ, S. 2012. Impact of precipitation dynamics on net ecosystem productivity. *Global Change Biology,* 18**,** 915-927.
PENDALL, E., HEISLER-WHITE, J. L., WILLIAMS, D. G., DIJKSTRA, F. A., CARRILLO, Y., MORGAN, J. A. & LECAIN, D. R. 2013. Warming reduces carbon losses from grassland exposed to elevated atmospheric carbon dioxide. *PloS one,* 8**,** e71921.
PIAO, S., CIAIS, P., FRIEDLINGSTEIN, P., PEYLIN, P., REICHSTEIN, M., LUYSSAERT, S., MARGOLIS, H., FANG, J., BARR, A. & CHEN, A. 2008. Net carbon dioxide losses of northern ecosystems in response to autumn warming. *Nature,* 451**,** 49-52.
PIAO, S., SITCH, S., CIAIS, P., FRIEDLINGSTEIN, P., PEYLIN, P., WANG, X., AHLSTRÖM, A., ANAV, A., CANADELL, J. G. & CONG, N. 2013. Evaluation of terrestrial carbon cycle models for their response to climate variability and to CO2 trends. *Global Change Biology,* 19**,** 2117-2132.
PLUMMER, M. Year. JAGS: A program for analysis of Bayesian graphical models using Gibbs sampling. *In:* Proceedings of the 3rd international workshop on distributed statistical computing, 2003. Technische Universit at Wien, 125.
POLLEY, H. W., BRISKE, D. D., MORGAN, J. A., WOLTER, K., BAILEY, D. W. & BROWN, J. R. 2013. Climate Change and North American Rangelands: Trends, Projections, and Implications. *Rangeland Ecology and Management,* 66**,** 493-511.

REICH, P. B., OLEKSYN, J. & WRIGHT, I. J. 2009. Leaf phosphorus influences the photosynthesis–nitrogen relation: a cross-biome analysis of 314 species. *Oecologia,* 160**,** 207-212.
REYES-FOX, M., STELTZER, H., TRLICA, M., MCMASTER, G. S., ANDALES, A. A., LECAIN, D. R. & MORGAN, J. A. 2014. Elevated CO2 further lengthens growing season under warming conditions. *Nature,* 510**,** 259-262.
RICHARDSON, A. D., BLACK, T. A., CIAIS, P., DELBART, N., FRIEDL, M. A., GOBRON, N., HOLLINGER, D. Y., KUTSCH, W. L., LONGDOZ, B. & LUYSSAERT, S. 2010a. Influence of spring and autumn phenological transitions on forest ecosystem productivity. *Philosophical Transactions of the Royal Society of London B: Biological Sciences,* 365**,** 3227-3246.
RICHARDSON, A. D., BLACK, T. A., CIAIS, P., DELBART, N., FRIEDL, M. A., GOBRON, N., HOLLINGER, D. Y., KUTSCH, W. L., LONGDOZ, B. & LUYSSAERT, S. 2010b. Influence of spring and autumn phenological transitions on forest ecosystem productivity. *Philosophical Transactions of the Royal Society B: Biological Sciences,* 365**,** 3227-3246.
RICHARDSON, A. D., KEENAN, T. F., MIGLIAVACCA, M., RYU, Y., SONNENTAG, O. & TOOMEY, M. 2013. Climate change, phenology, and phenological control of vegetation feedbacks to the climate system. *Agricultural and forest meteorology,* 169**,** 156-173.
ROY, J., MOONEY, H. A. & SAUGIER, B. 2001. *Terrestrial global productivity*, Academic Press.
RUSTAD, L., CAMPBELL, J., MARION, G., NORBY, R., MITCHELL, M., HARTLEY, A., CORNELISSEN, J. & GUREVITCH, J. 2001. A meta-analysis of the response of soil respiration, net nitrogen mineralization, and aboveground plant growth to experimental ecosystem warming. *Oecologia,* 126**,** 543-562.
RUSTAD, L. E. 2008. The response of terrestrial ecosystems to global climate change: towards an integrated approach. *Science of the Total Environment,* 404**,** 222-235.
RYAN, E. M., OGLE, K., ZELIKOVA, T. J., LECAIN, D. R., WILLIAMS, D. G., MORGAN, J. A. & PENDALL, E. 2015. Antecedent moisture and temperature conditions modulate the response of ecosystem respiration to elevated CO2 and warming. *Global Change Biology*.
SCHWINNING, S., SALA, O. E., LOIK, M. E. & EHLERINGER, J. R. 2004. Thresholds, memory, and seasonality: understanding pulse dynamics in arid/semi-arid ecosystems. *Oecologia,* 141**,** 191-193.
SHAW, M. R., ZAVALETA, E. S., CHIARIELLO, N. R., CLELAND, E. E., MOONEY, H. A. & FIELD, C. B. 2002. Grassland responses to global environmental changes suppressed by elevated CO2. *Science,* 298**,** 1987-1990.
SHERRY, R. A., WENG, E., ARNONE III, J. A., JOHNSON, D. W., SCHIMEL, D. S., VERBURG, P. S., WALLACE, L. L. & LUO, Y. 2008. Lagged effects of experimental warming and doubled precipitation on annual and seasonal aboveground biomass production in a tallgrass prairie. *Global Change Biology,* 14**,** 2923-2936.
SITCH, S., HUNTINGFORD, C., GEDNEY, N., LEVY, P., LOMAS, M., PIAO, S., BETTS, R., CIAIS, P., COX, P. & FRIEDLINGSTEIN, P. 2008. Evaluation of the terrestrial carbon cycle, future plant geography and climate-carbon cycle feedbacks using five Dynamic Global Vegetation Models (DGVMs). *Global Change Biology,* 14**,** 2015-2039.

SMITH, N. G., MALYSHEV, S. L., SHEVLIAKOVA, E., KATTGE, J. & DUKES, J. S. 2015. Foliar temperature acclimation reduces simulated carbon sensitivity to climate. *Nature Climate Change*.
SPIEGELHALTER, D. J., BEST, N. G., CARLIN, B. P. & VAN DER LINDE, A. 2002. Bayesian measures of model complexity and fit. *Journal of the Royal Statistical Society: Series B (Statistical Methodology),* 64**,** 583-639.
THORNLEY, J. H. 1976. *Mathematical models in plant physiology*, Academic Press (Inc.) London, Ltd.
WALKER, A. P., HANSON, P. J., DE KAUWE, M. G., MEDLYN, B. E., ZAEHLE, S., ASAO, S., DIETZE, M., HICKLER, T., HUNTINGFORD, C. & IVERSEN, C. M. 2014. Comprehensive ecosystem model-data synthesis using multiple data sets at two temperate forest free-air CO2 enrichment experiments: Model performance at ambient CO2 concentration. *Journal of Geophysical Research: Biogeosciences,* 119**,** 937-964.
WARING, R., LANDSBERG, J. & WILLIAMS, M. 1998. Net primary production of forests: a constant fraction of gross primary production? *Tree Physiology,* 18**,** 129-134.
WEBB, N. P., STOKES, C. J. & SCANLAN, J. C. 2012. Interacting effects of vegetation, soils and management on the sensitivity of Australian savanna rangelands to climate change. *Climatic Change,* 112**,** 925-943.
WILLIAMS, M., RASTETTER, E., FERNANDES, D., GOULDEN, M., WOFSY, S., SHAVER, G., MELILLO, J., MUNGER, J., FAN, S. & NADELHOFFER, K. 1996. Modelling the soil-plant-atmosphere continuum in a Quercus-Acer stand at Harvard Forest: the regulation of stomatal conductance by light, nitrogen and soil/plant hydraulic properties. *Plant, Cell & Environment,* 19**,** 911-927.
WILLIAMS, M., SCHWARZ, P. A., LAW, B. E., IRVINE, J. & KURPIUS, M. R. 2005. An improved analysis of forest carbon dynamics using data assimilation. *Global Change Biology,* 11**,** 89-105.
WITTIG, V. E., BERNACCHI, C. J., ZHU, X. G., CALFAPIETRA, C., CEULEMANS, R., DEANGELIS, P., GIELEN, B., MIGLIETTA, F., MORGAN, P. B. & LONG, S. P. 2005. Gross primary production is stimulated for three Populus species grown under free-air CO2 enrichment from planting through canopy closure. *Global Change Biology,* 11**,** 644-656.
ZAEHLE, S., MEDLYN, B. E., DE KAUWE, M. G., WALKER, A. P., DIETZE, M. C., HICKLER, T., LUO, Y., WANG, Y. P., EL-MASRI, B. & THORNTON, P. 2014. Evaluation of 11 terrestrial carbon–nitrogen cycle models against observations from two temperate Free-Air CO2 Enrichment studies. *New Phytologist,* 202**,** 803-822.
ZELIKOVA, T. J., WILLIAMS, D. G., HOENIGMAN, R., BLUMENTHAL, D. M., MORGAN, J. A. & PENDALL, E. 2015. Seasonality of soil moisture mediates responses of ecosystem phenology to elevated CO2 and warming in a semi-arid grassland. *Journal of Ecology,* 103**,** 1119-1130.

Tables 1-3 for Manuscript ID GCB-16-1419: Ryan, E. et al. ***Gross primary production responses to warming, elevated CO2, and irrigation:quantifying the drivers of ecosystem physiology in a semiarid grassland.*** **Global Change Biology.**

Table 1. Percent differences in predicted annual GPP for key pairs of treatments. Percentages are given for each year, for the six-year total (2007-2012), and for the six-year seasonal totals (spring, summer, fall). Asterisks denote the Bayesian P-value for the difference: $P \leq 0.01$ (**), $0.01 < P \leq 0.05$ (*) and $0.05 < P \leq 0.1$ ($^{(\dagger)}$). See Fig. 1 legend for treatment codes.

	2007	**2008**	**2009**	**2010**	**2011**	**2012**	**2007-2012**	**2007-2012 (Spring)**	**2007-2012 (Summer)**	**2007-2012 (Fall)**
Warming effect (cT - ct)	40**	30*	12	27$^{(\dagger)}$	50**	29	29*	129**	-11	56**
Elevated CO_2 effect (Ct - ct)	47**	31$^{(\dagger)}$	-5	7	49*	63**	26$^{(\dagger)}$	47$^{(\dagger)}$	1	124**
Warming and CO_2 effect (CT - ct)	28$^{(\dagger)}$	8	-11	-3	24$^{(\dagger)}$	-1	6	20	-5	42*
Deep irrigation effect (ctd - ct)	30*	30**	15	1	57**	61**	28**	31	19*	68**
Shallow irrigation effect (cts - ct)	29$^{(\dagger)}$	9	-10	-9	25$^{(\dagger)}$	41	9	2	2	66**

Table 2. Percent differences in predicted seasonal GPP for key pairs of treatments, for selected seasons. Pairs of treatments and seasons were selected based on the percent change values in the furthest three right columns of Table 1 that were significant (had asterisks). As in Table 1, asterisks denote the Bayesian P-value for the difference: $P \leq 0.01$ (**), $0.01 < P \leq 0.05$ (*) and $0.05 < P \leq 0.1$ ($^{(\dagger)}$). See Fig. 1 legend for treatment codes.

	2007	**2008**	**2009**	**2010**	**2011**	**2012**	**2007-2012**
Warming effect (cT – ct) for spring	109**	112**	70**	161**	209**	141**	129**
Warming effect (cT – ct) for fall	60**	27	146*	38	127**	97	56**
eCO_2 effect (Ct – ct) for fall	100**	46*	263**	281*	268**	461**	124**
eCO_2×warming effect (CT – ct) for fall	$45^{(\dagger)}$	7	129	89	90*	93	42*
Deep irrigation effect (ctd – ct) for summer	11	24*	11	-1	55**	27	19*
Deep irrigation effect (ctd – ct) for fall	$60^{(\dagger)}$	37*	$149^{(\dagger)}$	38	168**	$177^{(\dagger)}$	68**
Surface irrigation effect (cts – ct) for fall	44	-2	175**	208*	196**	315**	66**

Table 3. Summary of posterior estimates and Bayesian P-values for parameters in the A_{max} and Q functions (α's and β's, respectively; see Eqn. 3). Dark grey cells indicate $P \leq 0.001$, medium grey indicate $0.001 < P \leq 0.01$, light grey indicate $0.01 < P \leq 0.05$, and white indicate $P > 0.05$. The signs (+ or –) denote a positive or negative effect. See Fig. 1 legend for treatment codes.

Effect parameter (associated covariate)	**Treatment**					
	ct	**cT**	**Ct**	**CT**	**ctd**	**cts**
α_1 (SWC)	–			+		+
α_2 (VPD)	–					
α_3 (Tair)						
α_4 (SWC_{ant})		+		+		+
α_5 (VPD_{ant})		–	–	–	–	
α_6 ($Tair_{ant}$)		+	+	+	+	
α_7 (Nitrogen)			–			+
α_8 (Gness)	–				+	
α_9 ($Gness_{ant.diff}$)					–	
α_{10} (VPD×Tair)	+					
α_{11} (Tair×Tair)						
α_{12} (SWC×SWC_{ant})				–		–
α_{13} (Tair×$Tair_{ant}$)						
α_{14} (SWC_{ant}×$Tair_{ant}$)	+			+		
α_{15} (SWC_{ant}×VPD_{ant})	–			–		
β_1 (SWC)	+				+	–
β_2 (VPD)					–	
β_3 (Tair)						
β_4 (SWC_{ant})	+	+			+	
β_5 (VPD_{ant})						
β_6 ($Tair_{ant}$)	+	–				+
β_7 (Gness)	+					
β_8 ($Gness_{ant.diff}$)						
β_9 (VPD×Tair)						
β_{10} (Tair×Tair)		+				
β_{11} (SWC×SWC_{ant})				+		
β_{12} (Tair×$Tair_{ant}$)						
β_{13} (SWC_{ant}×$Tair_{ant}$)		–		–	–	+
β_{14} (SWC_{ant}×VPD_{ant})	+			+	+	

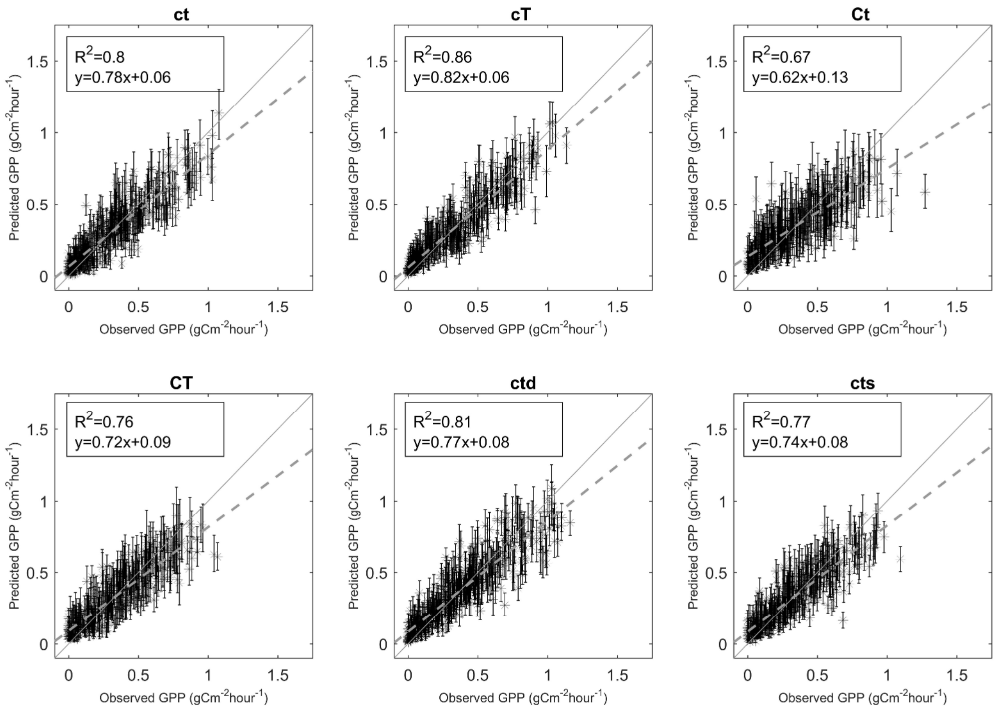

Observed versus predicted GPP for each treatment. The predicted values were obtained from the main model (with antecedent effects) and are represented by the posterior means and central 95% credible intervals of replicated observations (Gelman et al., 2013) of GPP, based on Eqns (1) and (2). The solid, diagonal gray line represents the 1:1 line; the dashed line represents the best fit line. Treatment codes involve combinations of: c (ambient CO2), C (elevated CO2), t (no warming), T (warming), d (deep irrigation), or s (shallow irrigation).

Fig. 1

1381x985mm (96 x 96 DPI)

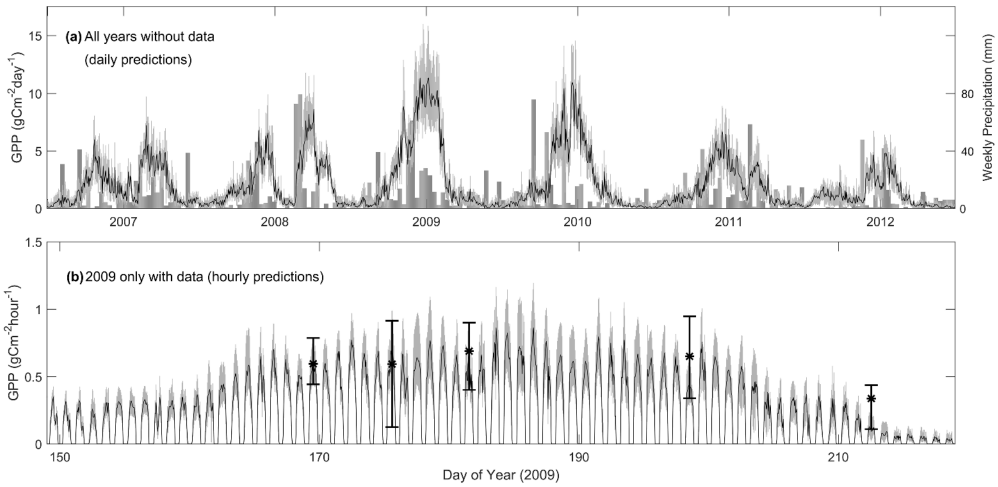

Time-series of predicted gross primary production (GPP) for (a) daily GPP for the control (ct) treatment, where the grey bars denote the weekly precipitation at the site, and (b) hourly GPP for days of the year 140-215 for 2009 for the ct treatment (observed GPP is denoted by *). In both (a) and (b), the black line represents the posterior mean of the daily (a) or hourly (b) predicted GPP, and the grey error bars indicate the 95% credible intervals. The data points and associated error bars in panel (b) represent the mean and range of GPP observations made on measurement days and across at least four of the five plots of the control treatment.
Fig. 2
1927x930mm (96 x 96 DPI)

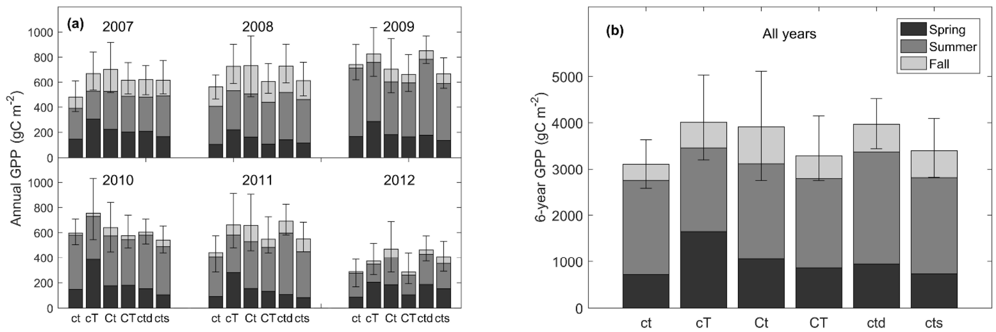

Predicted annual (growing season; March-October) and seasonal GPP for each treatment by (a) each study year and (b) summed across all six years. The overall height of each bar denotes the posterior mean and the error bars represent the central 95% credible intervals of the (a) annual GPP or (b) six-year GPP. The totals represented by each bar are broken-down by seasonal totals according to the shading. See Fig. 1 legend for treatment codes.

Fig. 3

1879x644mm (96 x 96 DPI)

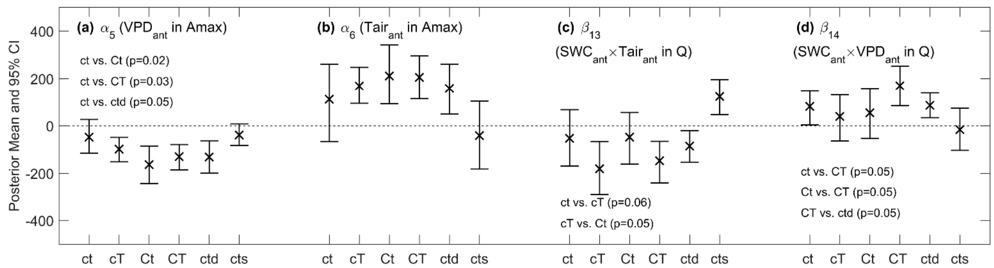

Posterior means (denoted by ×) and central 95% credible intervals (CIs; error bars) for a subset of parameters (covariate effects) in the Amax function (panels a and b) and the Q function (panels c and d) (Eqn. 3, Table 2); these parameters were the most significant across the greatest number of treatments. The key Amax parameters are associated with antecedent vapor pressure deficit (VPDant) and antecedent air temperature (Tairant). The key Q parameters are associated with antecedent soil water content (SWCant) and the interaction between SWCant and VPDant. 95% CIs that overlap with zero (dashed horizontal line) indicate a non-significant effect. See Fig. 1 legend for treatment codes.

Fig. 4

1883x519mm (96 x 96 DPI)

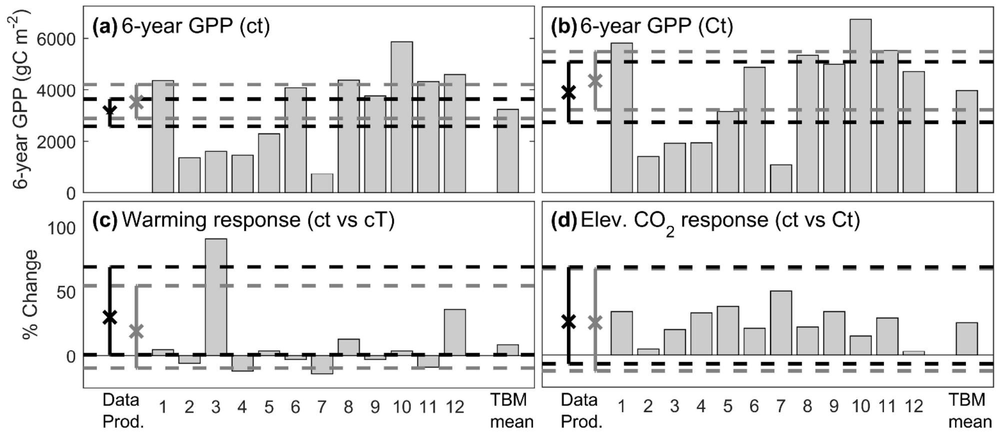

Comparison of the posterior estimates of GPP ('data product'; × = posterior mean; error bars and horizontal dashed lines = 95% credible interval) with simulated GPP from 12 terrestrial biosphere models (TBMs; see Table S1 in the supplementary information for descriptions of each TBM, labeled 1-12). The GPP data products are based on the GPP posterior estimates generated from the main (black lines and symbols) and alternative (gray lines and symbols) models, where the alternative model is the same as the main model but without antecedent effects. The metrics shown here are: total six year GPP (2007-2012; growing season, March-October in each year) under (a) the control (ct) treatment and (b) the elevated CO2 (Ct) treatment; and, percentage change in total six year GPP under (c) warming (cT) relative to ct, and (d) Ct relative to ct.
Fig. 5
1239x551mm (96 x 96 DPI)